J Appl Electrochem (2010) 40:493–497
DOI 10.1007/s10800-009-0020-2

ORIGINAL PAPER

Ionic liquid assisted one step green synthesis of Au–Ag bimetallic nanoparticles

Tsung-Hsuan Tsai · Soundappan Thiagarajan · Shen-Ming Chen

Received: 4 May 2009 / Accepted: 25 September 2009 / Published online: 10 October 2009

Abstract Au–Ag bimetallic nanoparticles have been fabricated by one-step simple electrochemical deposition method using ionic liquid as green electrolyte (1-butyl-3-methylimidazolium tetrafluoro borate). Fabricated Au–Ag bimetallic nanoparticles have been characterized using cyclic voltammetry (CV), FE-SEM, UV–vis spectroscopy, and X-ray diffraction (XRD) studies. The electrodeposited Au–Ag bimetallic nanoparticles were found in the size range of 16–30 nm, respectively. This type of Au–Ag bimetallic nanoparticles could be directly applied for the optoelectronic and biosensing applications.

Keywords Green synthesis · Bimetallic nanoparticles · Ionic liquid · Electro deposition · Cyclic voltammetry

1 Introduction

Shape-controlled nanomaterial fabrications have been found as imperative research in optical, electronic, and biosensor applications [1, 2]. Especially, utilization of ionic liquids (ILs) as green electrolytes for the fabrication of nanomaterials is found as new one in green chemistry [3, 4]. For example, ILs employed green synthesis of gold [5, 6]; silver [7]; nickel [8]; palladium [9]; Cr, Mo, and W nanoparticles [10]; Ag–Au alloy nano structures [11, 12]; TiO_2 nano tubulars [13]; cobalt nano wires [14]; and aluminum nanorods [15] has been reported. The development of two-dimensional (2D) metal nanostructures [16–29]; triangular Au core–Ag shell nanoparticles [30], and multi-shell bimetallic AuAg nanoparticles [31]; synthesis, characterization, and SERS activity of Au–Ag nanorods [32]; Au–Ag alloy nanoparticles with Au/Ag compositional control in SiO_2 film matrix [33]; photo-induced self-assembly of Au–Ag–Hg trimetallic nanoparticles from glycine solution [34]; and cyanobacteria assisted synthesis of Au, Ag, Pd, and Pt nanoparticles via an enzyme-mediated route [35] has been extensively studied because of their remarkable abilities in the wide range of applications. All these literature surveys clearly show number of methods for the fabrication of monometallic, bimetallic nanomaterials and suggest the green synthesis as a new pathway for the fabrication of nanomaterials. Thus, here we have focused on green synthesis and attempted to fabricate the nanomaterials using the ILs as green electrolytes. For the first time, we are reporting a novel and simple one-step electrochemical deposition process using ILs as green electrolytes for the fabrication of Au–Ag bimetallic nanoparticles. The indium tin oxide (ITO) surface has been utilized for the fabrication of Au–Ag bimetallic nanoparticles. Au–Ag bimetallic modified ITO has been characterized using FE-SEM, UV–visible spectroscopy, and X-ray diffraction analysis.

2 Experimental

2.1 Chemicals

$AgClO_4$ (97%) and $KAuCl_4 \cdot 3H_2O$ were purchased from Sigma–Aldrich and Strem chemicals (USA). Room temperature IL (1-butyl-3-methylimidazolium tetrafluoro borate) (97%) was purchased from Fluka (Sigma–Aldrich,

T.-H. Tsai · S. Thiagarajan · S.-M. Chen (✉)
Electroanalysis and Bioelectrochemistry Laboratory,
Department of Chemical Engineering and Biotechnology,
National Taipei University of Technology, No. 1, Section 3,
Chung-Hsiao East Road, Taipei 106, Taiwan, ROC
e-mail: smchen78@ms15.hinet.net

Switzerland) and used without further purification. ITO-coated transparent conducting glass plates (3 × 1 cm) with the resistivity of 80 Ω cm^{-1} were used as working electrodes. ITO glass surfaces were washed with a solution of Triton X-100 and sonicated with deionized water and ethanol for 10 min. Other chemicals (Merck) used in this investigation were of analytical grade. Double distilled deionized water was obtained from a Millipore Alpha-Q Lotun ultrapure water system. All the experimental results have been obtained at room temperature. A phosphate buffer solution (PBS) (0.1 M, pH 7) was prepared using NaH_2PO_4–Na_2HPO_4. Pure nitrogen was passed through all the experimental solutions.

2.2 Apparatus

Electrochemical experiments were performed using CHI1205a, electrochemical workstation (CH Instruments, Austin, USA). A conventional three-electrode system was used for the electrochemical deposition process which consists of ITO glass plate as working and Ag wire filled with (1-butyl-3-methylimidazolium tetrafluoro borate) Ag/IL as a reference and platinum wire as counter electrode. Remaining electrochemical experiments have been done using Ag/AgCl reference electrode (3 mol L^{-1} KCl). All the experiments have been conducted at room temperature. FE-SEM images were obtained using JEOL JSM-6700F (JEOL Ltd, Japan). UV–visible spectra were obtained using Hitachi U-3300 spectrophotometer (Japan). The XRD experiment was done using XPERT-PRO (PANalytical B.V., The Netherlands) diffractometer using Cu Kα radiation ($\lambda = 1.54$ Å). The samples were scanned in the range of 10–80° (2θ).

2.3 Fabrication of Au–Ag bimetallic nanoparticles

Surface-cleaned ITO glass plates have been placed in 1 mL 1-butyl-3-methylimidazolium tetrafluoro borate containing 1 mM $KAuCl_4{\cdot}3H_2O$ and $AgClO_4$. Here, cyclic voltammetry (CV) technique has been employed for the electrochemical deposition process. Au–Ag bimetallic nanoparticles were directly deposited on ITO surface by applying a repetitive potential scan between 1.0 and −1.0 V (vs. Ag/IL) at the scan rate of 0.05 V s^{-1} for five cycles. Further, the Au–Ag bimetallic nanoparticle-modified ITO was carefully washed with distilled water and completely dried and employed for the further detailed analysis.

3 Results and discussion

Figure 1 shows the characteristic CVs of Au–Ag nanoparticles electro deposition process which starts at the positive potential 1.0 V and ends in the negative potential −1.0 V at the scan rate of 0.05 V s^{-1} (vs. Ag/IL) for five cycles. Here, the reduction of Au occurs at peak 1(a) at the potential of −0.17 V and extends up to −0.82 V [peak 2(a)], where the peak current is higher in the first scanning. This shows that at initial, the nucleation of Au(I) occurs and requires over potential (−0.82 V) for the electro deposition of Au (0). In the following cycles, this peak current decreases and initiates at −0.81 V [peak 3(a)]. During the continuous cycling process, the growth of reduction peaks at −0.17, −0.81, and −0.50 V [peak 1(b)] confirms the electro deposition of Au–Ag bimetallic nanoparticles on the ITO glass surface. Further, the oxidation peaks around 0.12 and 0.58 V indicate the oxidation of chloride to chlorine [36, 37]. Based on previous literature reports, the expected mechanism for the formation of Au (0) and Ag (0) electrodeposition processes are as follows [36–38]:

$$[AuCl_4]^- + 2e^- \rightarrow [AuCl_2]^- + 2Cl^- \quad (1)$$

$$[AuCl_2]^- + e^- \rightarrow Au(0) + 2Cl^- \quad (2)$$

$$AgClO_4 \rightarrow Ag^+ + ClO_4^- \quad (3)$$

$$Ag^+ + e^- \rightarrow Ag^0 \quad (4)$$

Next, the Au–Ag nanoparticle-modified ITO was immersed in pH 7.0 PBS for the further electrochemical studies. Here, the cyclic voltammogram (inset of Fig. 1) clearly shows the two reduction peaks of Au and Ag at around 0.48 and 0.07 V, respectively. The oxidation peak of Ag exhibits at around 0.31 V. This result clearly resembles the presence of electrodeposited Au–Ag nanoparticles on the ITO surface. In the next step, the Au–Ag bimetallic nanoparticle-modified ITO glass surface has

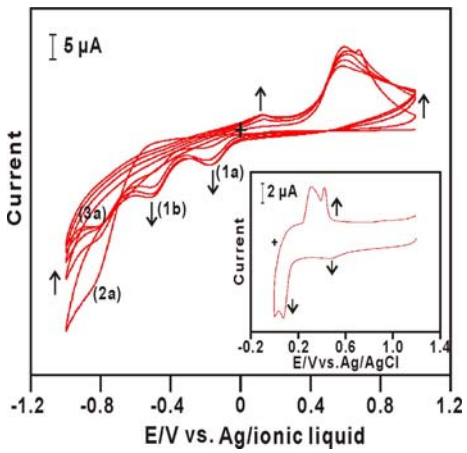

Fig. 1 Consecutive cyclic voltammograms of Au–Ag bimetallic nanoparticles electrodeposition on ITO glass surface [1 mM $KAuCl_4{\cdot}3H_2O$ and $AgClO_4$ dissolved in ionic liquid (1-butyl-3-methylimidazolium tetrafluoro borate)] at the scan rate of 0.05 V s^{-1} for five cycles. *Inset* show the cyclic voltammogram of the electrodeposited Au–Ag on ITO (in pH 7.0 PBS)

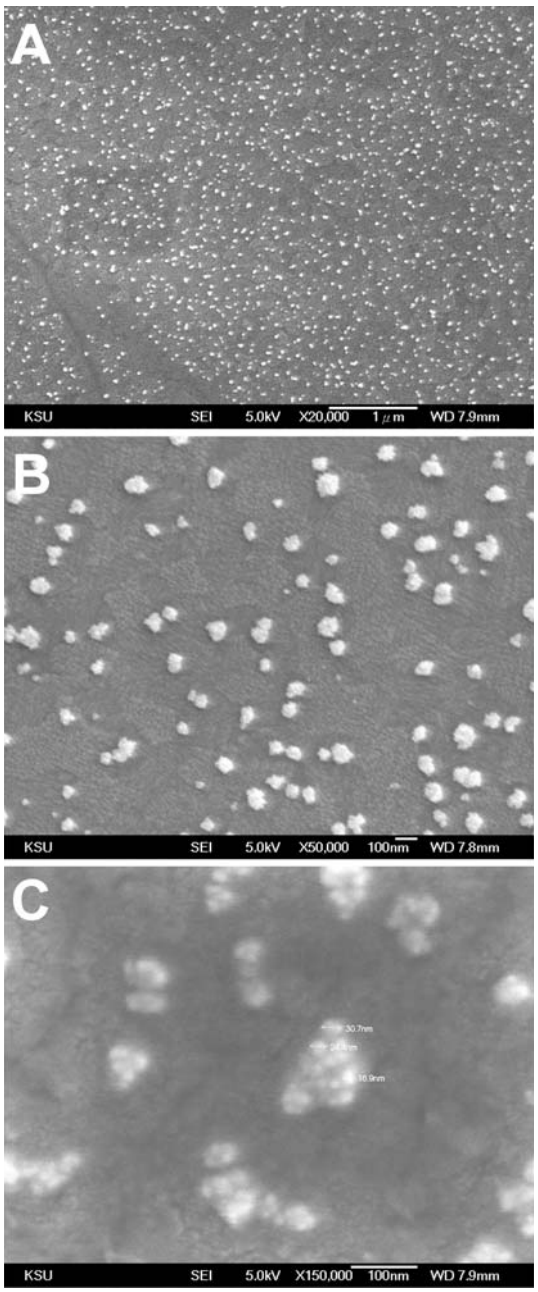

Fig. 2 FE-SEM images of Au–Ag bimetallic nanoparticles modified ITO. Magnification: **a** ×20,000 (5 KV), **b** ×50,000 (5 KV) and **c** ×150,000 (5 KV)

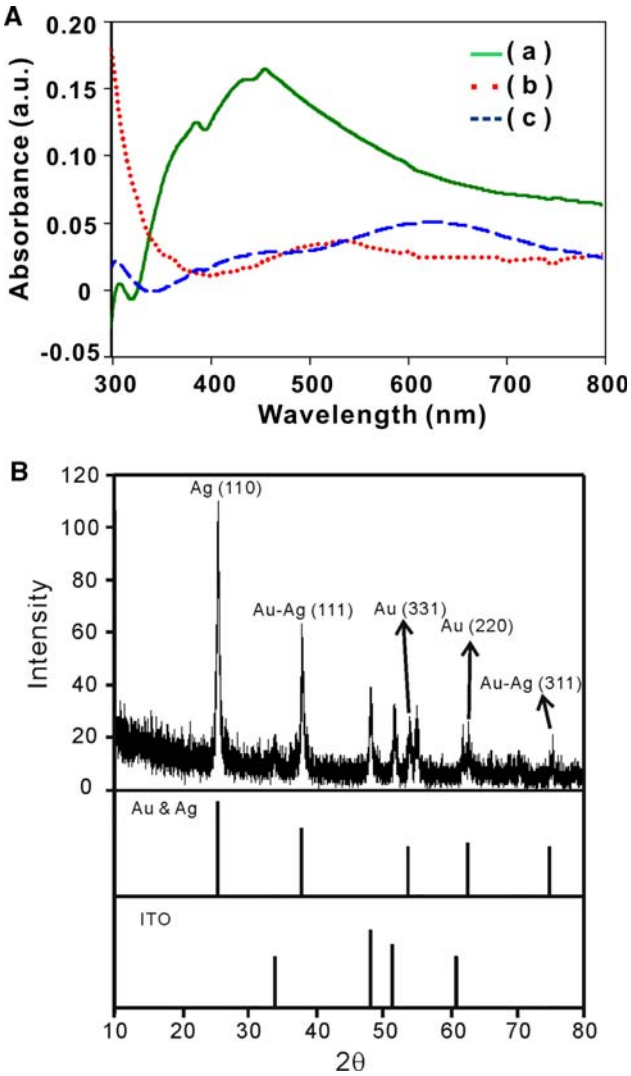

Fig. 3 **a** UV–vis absorption spectra of (*a*) Ag, (*b*) Au and (*c*) Au–Ag bimetallic nanoparticles modified ITO, **b** X-ray diffraction pattern of Au–Ag bimetallic nanoparticles modified ITO

been employed for the FE-SEM analysis. Figure 2a shows the large scale view [20,000× (5 KV)] of electrodeposited Au–Ag bimetallic nanoparticles on ITO. Figure 2b and c show the magnified views (50,000× and 150,000×) of the electrodeposited Au–Ag bimetallic nanoparticles. Based on Fig. 2b and c, we can clearly see that the electrodeposited

Table 1 Comparison table for bimetallic nanoparticles synthesis utilizing ionic liquids

S. no.	Ionic liquid/method	Type of nanoparticles	Particle size range (nm)	Ref
1.	$BMIMPF_6$/sputter deposition technique	AuAg	2–10	[11]
2.	(a) $BMIMPF_6$/chemical synthesis	PdAu	6.0 ± 2.9	[39]
	(b) $BMIMPF_6$ (in the presence of additive1-methylimidazole)	PdAu	3.0 ± 0.5	
3.	BMI/electrochemical deposition	Au–Ag	16–30	This work

BMIMPF$_6$ 1,3-butylmethylimidazolium hexafluorophosphate

BMI 1-butyl-3-methylimidazolium tetrafluoro borate

Table 2 Comparison table for AuAg nanoparticles synthesis based on other general methods

S. no.	Method	Type of nanoparticles	Size (nm)	Ref
1.	Chemical synthesis (oleic acid)	AuAg	8–9	[40]
2.	Sol–gel process	Au–Ag alloy	1–6	[41]
3.	Chemical synthesis	AuAg	2–7	[42]
4.	LVCC	Au–Ag alloy	10–60	[43]
5.	Electrochemical co-reduction	Au–Ag alloy	11	[44]
6.	BMI/electrochemical deposition	Au–Ag	16–30	This work

LVCC laser vaporization controlled condensation

Au–Ag nanoparticles have been gathered together and resemble like a flower-shaped one, respectively. Further, the minimum and maximum size ranges of the Au–Ag bimetallic nanoparticles have been found as 16, 24, and 30 nm. Here, the maximum size range of Au–Ag bimetallic nanoparticles was found to be 92 nm. Finally, the FE-SEM result clearly validates the presence of Au–Ag of bimetallic nanoparticles on the ITO surface.

In the next step, UV–visible spectroscopy and XRD analysis have been employed to verify and validate the Au–Ag bimetallic nanoparticles modified ITO. Figure 3a shows the UV–visible absorption spectra for electrodeposited Ag, Au nano particles and Au–Ag bimetallic nanoparticles modified ITO. For the electrodeposited Ag particles, a strong UV absorption peak centered at 450 nm has been noticed corresponds to the presence of Ag particles on the ITO surface. For only Au, UV absorption peak appears at 530 nm, which validates the presence of Au particles. At the same time, for Au–Ag bimetallic nanoparticles deposition, the corresponding Ag and Au absorption peaks appear at 440 and 620 nm. Therefore, the absorption peak shift (of Ag and Au) clearly validates the bimetallic nature of Au–Ag nanoparticles. Finally, the UV-spectrum studies clearly represent the presence of both Ag and Au nanoparticles and validate the bimetallic structure of the Au–Ag nanoparticles, respectively. Further XRD has been employed to validate the proposed Au–Ag bimetallic nanoparticles on the ITO glass substrate. Figure 3b shows the XRD pattern obtained for the Au–Ag nanoparticles modified ITO. Here, five different characteristic peaks obtained were Ag (110), Au–Ag (111), Au (331), Au (220), and Au–Ag (311). All these five XRD peaks clearly validate the presence of Au–Ag bimetallic nanoparticles on the ITO surface. Next, the proposed method has been compared with previous literature reports. Here, Tables 1 and 2 represent IL and general method based comparison study for the bimetallic nanoparticles synthesis process. From these two comparison tables, we can conclude a decision that IL-based electrochemical fabrication results in the formation of higher size range Au–Ag bimetallic nanoparticles. However, the specific advantage of this method is the one step easy electrochemical fabrication of Au–Ag bimetallic nanoparticles. This is the most important advantage of this method comparing with the other general methods, respectively.

4 Conclusion

In summary, we have successfully employed one-step simple electrochemical deposition method using IL as green electrolyte for the fabrication of Au–Ag bimetallic nanoparticles. Fabricated Au–Ag bimetallic nanoparticles were well characterized using CV, FE-SEM, UV–vis spectroscopy, and XRD analysis. The great advantage of our method is using IL as a green electrolyte which minimizes the interest of using hazardous chemicals and solvents for the nanomaterials fabrication process. Also, the user friendly, easily accessible, very simple, and a novel one-step simple electrochemical deposition method which can be adoptable one for all kind of researchers in easy manner to synthesize the bimetallic nanoparticles. The proposed Au–Ag bimetallic nanoparticles could be directly applied for opto-electronic, biosensor, and various different types of applications. Further, a detailed investigation on Au–Ag bimetallic nanoparticles modified electrodes for the electrochemical biosensor applications is currently ongoing research in our laboratory.

Acknowledgment This work was supported by grants from National Science Council (NSC) and the Ministry of Education of the Taiwan (ROC).

References

1. McFarland AD, Van Duyne RP (2003) Nano Lett 3:1057
2. Amanda JH, Chang L, William KL, Richard PV (2005) J Am Chem Soc 127:2264
3. Abedin S, Pölleth M, Meiss SA, Janek J, Endres F (2007) Green Chem 9:549
4. Dahl JA, Maddux BLS, Hutchison JE (2007) Chem Rev 107:2228
5. Wang Z, Zhang Q, Kuehner D, Ivaska A, Niu L (2008) Green Chem 10:907

6. Itoh H, Naka K, Chujo Y (2004) J Am Chem Soc 126:3026
7. Li N, Bai X, Zhang S, Gao Y, Zheng L, Zhang J, Ma H (2008) J Dispers Sci Technol 29:1059
8. Migowski P, Machado G, Texeira S, Alves M, Morais J, Traversec A, Dupont J (2007) Phys Chem Chem Phys 9:4814
9. Ou G, Xu L, He B, Yuan Y (2008) Chem Commun 35:4210
10. Redel E, Thomann R, Janiak C (2008) Chem Commun 15:1789
11. Okazaki K, Kiyama T, Hirahara K, Tanaka N, Kuwabata S, Torimoto T (2008) Chem Commun 6:691
12. Bhatt A, Mechler A, Martina L, Bond A (2007) J Mater Chem 17:2241
13. Paramasivam I, Macaka JM, Selvam T, Schmuki P (2008) Electrochim Acta 54:643
14. Yang P, An M, Su C, Wang F (2008) Electrochim Acta 54:763
15. Perre E, Nyholm L, Gustafsson T, Taberna P, Simon P, Edström K (2008) Electrochem Commun 10:1467
16. Callegari A, Tonti D, Chergui M (2003) Nano Lett 3:1565
17. Yin Y, Alivisatos P (2005) Nature 437:664
18. Jin RC, Cao YW, Mirkin CA, Kelly KL, Schatz GC, Zheng JG (2005) Science 294:1901
19. Jin RC, Cao YW, Metraux GS, Schatz GC, Mirkin CA (2001) Nature 425:487
20. Santos IP, Marzan LM (2002) Nano Lett 2:903
21. Metraux GS, Cao YW, Jin RC, Mirkin CA (2003) Nano Lett 3:519
22. Santos IP, Marzán LM (2008) J Mater Chem 18:1724
23. Iyer KS, Bond CS, Saunders M, Raston CL (2008) Cryst Growth Des 8:1451
24. Yang Y, Matsubara S, Xiong L, Hayakawa T, Nogami M (2007) J Phys Chem C 111:9095
25. Sajanlal PR, Pradeep T (2008) Adv Mater 20:980
26. Shankar SS, Rai A, Ankamwar B, Singh A, Ahmad A, Sastry M (2004) Nat Mater 3:482
27. Shankar SS, Rai A, Ahmad A, Sastry M (2005) Chem Mater 17:566
28. Haes AJ, Zhao J, Zou S, Own CS, Marks LD, Schatz GC, Duyne RPV (2005) J Phys Chem B 109:11158
29. Haes AJ, Duyne RPV (2002) J Am Chem Soc 124:10596
30. Rai A, Chaudhary M, Ahmad A, Bhargava S, Sastry M (2007) Mater Res Bull 42:1212
31. González BR, Burrows A, Watanabe M, Kiely CJ, Marzán LL (2005) J Mater Chem 15:1755
32. Daizy Philip KJ, Gopichandran C, Unni KM (2008) Spectrochim Acta A 70:780
33. Pal S, De D (2007) J Nanosci Nanotechnol 7:1994
34. Huang YF, Huang KM, Chang HT (2007) J Nanosci Nanotechnol 7:3172
35. Barberousse BR, Hemadi H, Djedjat M, Yéprémian C, Coradin C, Livage T, Fiévet J, Couté F (2007) J Nanosci Nanotechnol 7:2696
36. Aldous L, Silvester DS, Villagrán C, Pitner WR, Compton RG, Lagunas MC, Hardacre C (2006) New J Chem 30:1576
37. Aldous L, Silvester DS, Pitner WR, Compton RG, Lagunas MC, Hardacre C (2007) J Phys Chem C 111:8496
38. Oyama T, Okajima T, Ohsaka T (2007) J Electrochem Soc 154:322
39. Dash P, Scott RWJ (2009) Chem Commun 812–814. doi: 10.1039/b816446k
40. Wang C, Yin H, Chan R, Peng S, Dai S, Sun S (2009) Chem Mater 2(1):433
41. Supriya D, Bera P, Sampath S (2005) J Colloid Interface Sci 290:117
42. Han SW, Kim Y, Kim K (1998) J Colloid Interface Sci 208:272
43. Abdelsayed V, Saoud KM, Samy El-Shall M (2008) J Nanopart Res 8:519
44. Zhou M, Chen S, Zhao S, Ma H (2006) Physica E 33:28